

An Uplink Control Channel Design with Complementary Sequences for Unlicensed Bands

Alphan Şahin, *Member, IEEE*, and Rui Yang, *Member, IEEE*

Abstract—In this study, we propose two schemes based on non-contiguous complementary sequences (CSs) for the uplink control channels in unlicensed bands. The first scheme is designed for non-coherent detectors and allows the users to transmit 1-2 bit information via CSs. This scheme addresses two complicated problems, i.e., minimization of peak-to-average-power ratio (PAPR) and multi-access interference, without introducing trade-off between them. The second scheme exploits the generic CS encoder and enables at least 21 information bits for a single user or 11 bits/user for three users on the same frequency resources, respectively, while limiting the PAPR to a maximum of 3 dB for an orthogonal frequency division multiplexing (OFDM) symbol. To derive the proposed schemes, we use an extension of Golay's concatenation and interleaving methods. We obtain a new theorem which leads to a CS encoder compatible with a wide variety of non-contiguous resource allocations. The numerical results show that the proposed schemes maintain the PAPR benefits without increasing the error rate for non-contiguous resource allocations in the frequency domain.

Index Terms—Control channels, complementary sequences, PAPR, Reed-Muller code, OFDM, unlicensed spectrum

I. INTRODUCTION

In recent years, significant growth in mobile broadband services has led to a dramatic increase in data traffic and a high demand for more spectrum. While improving the efficiency of mobile network operations over licensed spectrum, cellular network operators have also started utilizing the unlicensed spectrum via Wi-Fi offloading [1]. To provide seamless network connectivity and improve the efficiency of overall networks over both licensed and unlicensed bands, wireless system designers and network operators in standard organizations have made significant efforts to enable the communication protocols designed for licensed bands work in unlicensed bands.

Physical layer design for communication on unlicensed bands face a set of challenges which are different from the ones on licensed bands as more stringent regulatory requirements on unlicensed bands exist to ensure spectrum is shared fairly and coexistence is allowed among different radio access technologies. These requirements limit the freedom of resource allocation in orthogonal frequency division multiple access (OFDMA) based systems. For example, according to the ETSI regulations [2], in the 5 GHz band, the power spectral density (PSD) of the transmitted signal should be less than

The material in this work has appeared in part at the 2019 IEEE International Communications Conference (ICC). Alphan Şahin and Rui Yang are affiliated with University of South Carolina, Columbia, SC and InterDigital, Huntington Quadrangle, Melville, NY, respectively. E-mail: asahin@mailbox.sc.edu, rui.yang@interdigital.com

10 dBm/MHz and the occupied channel bandwidth (OCB) should be larger than 80% of the nominal channel bandwidth. Therefore, a narrow bandwidth transmission (e.g., 180 kHz resource block (RB) in 3GPP Long-Term Evolution (LTE)) in 20 MHz channel in a 5 GHz unlicensed band does not meet the OCB requirement and limits the coverage range due to the PSD requirement. To be able to increase the transmit power under the PSD constraint while complying with the OCB requirement, today's major communication standards such as 3GPP LTE enhanced licensed-assisted access (eLAA) and NR in unlicensed spectrum (NR-U) have adopted an interlaced allocation scheme [3] which allocates disperse and non-contiguous RBs, called an *interlace*, for each link.

Non-contiguous resource allocation in the frequency domain is a well-known method to enhance the reliability of a link via frequency diversity gain. However, it can potentially make the high peak-to-average-power ratio (PAPR) issue in orthogonal frequency division multiplexing (OFDM) signals even worse [4], which would be a major concern for uplink transmissions. This issue can also be a detrimental factor for reliability, transmission power efficiency, and coverage range, particularly when the transmission needs to be limited to only one or two OFDM symbols for latency reduction.

In the literature, there are numerous approaches investigating PAPR challenge for OFDM [5]. For example, with partial transmit sequences (PTS) [6], additional phase rotations are applied to the symbol groups in frequency such that the resulting signal has low PAPR. However, PTS can increase the overhead as the receiver may need to know the rotations. Companding transform is another widely-used method which compensates the distortion due to the hardware non-linearity at the expense of higher bit-error rate (BER) [7]. Another approach is discrete Fourier transform (DFT) precoding [8], i.e., DFT-spread OFDM, where the multicarrier structure of a plain OFDM symbol is effectively converted to a wideband single carrier waveform [9]. It substantially decreases the fluctuations in time when the resource allocation is contiguous in the frequency and low-order modulation symbols are utilized. It also admits several methods such as frequency domain windowing to decrease the PAPR further [10]. On the other hand, in cases of non-contiguous resource allocation after DFT precoding, the low-PAPR benefit of DFT-spread OFDM diminishes as it loses its single carrier structure. The approaches that take the encoding into account for reducing PAPR may require a joint design that typically imposes additional constraints on coding structure, modulation type, and waveform parameters such as resource allocation. For example, obtaining parity bits exhaustively that leads to low PAPR [11] or using offsets from

linear code [12] are several methods that place constraints on the parity bits. In [13], Daoud and Alani proposed to use low-density parity check (LDPC) codes to mitigate the PAPR of OFDM symbols via exhaustive search. In [14], various interleavers were proposed for Turbo encoder to reduce the PAPR. To mitigate PAPR via encoding, a remarkable method has been established with complementary sequences (CSs) [15], especially after the connection between CSs and Reed-Muller (RM) codes was discovered by Davis and Jedwab [16]. However, synthesizing CSs for a given resource allocation, e.g., NR-U interlace, is a challenging task. Recently, a theoretical framework was proposed to synthesize CSs with null symbols, i.e., non-contiguous CS, where the number of non-zero elements is $2^m \cdot N$ [17] for non-negative integer m and N . Therefore, it is still not trivial to synthesize non-contiguous CSs compatible with 3GPP LTE eLAA or NR-U interlace.

In 3GPP 5G New Radio (NR) R15, five formats for the uplink control channel are adopted for the licensed bands [18]. Format 0 is a sequence-based design which enables a non-coherent detection at the receiver for 1-2 bit transmission (e.g., such as ACK/NACK signaling) on a single RB. The same design is extended to another format, i.e., Format 1, by repeating the sequences for Format 1 over multiple OFDM symbols, which increases the coverage range. The reliability of 1-2 bit uplink control information is improved by the sequences that lead to low PAPR. Format 2-4 support medium payloads (i.e., 2-11 bits) with a linear block code and large payloads (i.e., more than 11 bits) with a polar code to enhance the reliability. While Format 2 and Format 3 are constructed with 1-2 and 4-14 OFDM symbols, respectively, with flexible number of RBs, Format 4 is based on 4-14 DFT-spread OFDM symbols only for single RB. A similar formatting strategy for the uplink control channel in the unlicensed bands can also be beneficial for addressing different needs of network. However, as discussed in Section II-B, the non-contiguous resource allocation in the unlicensed bands is a major constraint for a low PAPR design, which prohibits the straightforward extensions of the NR R15 uplink control channel formats, particularly for a small or medium payloads. For this reason, in this study, we focus on the low-PAPR design for a small or medium payloads within a single OFDM symbol while supporting multiple users on the same interlace.

In this study, we build on our initial work in [19] which investigates two CS-based schemes for 1-2 bit transmission for unlicensed bands. We extend our previous work by addressing the issue of supporting a larger payload with CSs, brought up in [19]. We propose a new scheme which allow a user to transmit a larger payload on an interlace, based on non-contiguous CSs. We obtain a new theorem, i.e., Theorem 2, which provides a large number of distinct non-contiguous Golay complementary pair (GCP) compatible with an NR-U interlace, by exploiting the framework proposed in [17]. The proposed scheme exploits the properties of Theorem 2 and yields an OFDM symbol that enables at least 21 information bits for a single user or 11 bits/user for three users on the same interlace.

The rest of the paper is organized as follows. In Section II, we set the notation and provide preliminary discussions

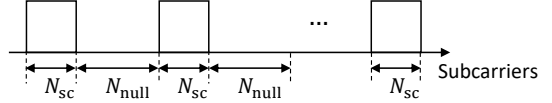


Figure 1. Interlace model.

on sequences. In Section III, we provide our main theorem, i.e., Theorem 2, and obtain the proposed scheme for larger payloads. We also capture our CS-based scheme for 1-2 bit transmission for non-coherent receivers [19] in Section III. In Section IV, we present numerical results and compare the proposed schemes with other potential approaches. We conclude the paper in Section V.

Notation: The field of complex numbers, the set of integers, and the set of positive integers are denoted by \mathbb{C} , \mathbb{Z} , and \mathbb{Z}^+ , respectively. The symbols i , j , $+$, and $-$ denote $\sqrt{-1}$, $-\sqrt{-1}$, 1, and -1 , respectively. A sequence of length N is represented by $\mathbf{a} = (a_n)_{n=0}^{N-1} = (a_0, a_1, \dots, a_{N-1})$. The element-wise complex conjugation and the element-wise absolute operation are denoted by $(\cdot)^*$ and $|\cdot|$, respectively. The conjugate reflecting reverses the order of the elements of \mathbf{a} and applies element-wise complex conjugation, denoted by $\tilde{\mathbf{a}}$. The operation $\uparrow_k \{\mathbf{a}\}$ introduces $k-1$ null symbols between the elements of \mathbf{a} . The operations $\mathbf{a} + \mathbf{b}$, $\mathbf{a} - \mathbf{b}$, $\mathbf{a} \odot \mathbf{b}$, $\mathbf{a} * \mathbf{b}$, and $\langle \mathbf{a}, \mathbf{b} \rangle$ are the element-wise summation, the element-wise subtraction, the element-wise multiplication, linear convolution, and the inner product of \mathbf{a} and \mathbf{b} , respectively.

II. PRELIMINARIES AND FURTHER NOTATION

A. Interlace

We model an interlace as a non-contiguous resource allocation which consists of N_{rb} RBs each of which composed of N_{sc} subcarriers where the RBs are separated by N_{null} tones in the frequency domain as illustrated in Figure 1. The interlace in LTE eLAA can be expressed as $N_{\text{sc}} = 12$ subcarriers, $N_{\text{rb}} = 10$ RBs, and $N_{\text{null}} = 9 \times 12 = 108$ subcarriers. In NR-U, the interlace structure can vary based on the subcarrier spacing, e.g., 15, 30, or 60 kHz, and bandwidth, e.g., 20, 40, or 80 MHz.

B. Polynomial Representation of a Sequence

The polynomial representation of the sequence \mathbf{a} can be given by

$$p_{\mathbf{a}}(z) \triangleq a_{N-1}z^{N-1} + a_{N-2}z^{N-2} + \dots + a_0, \quad (1)$$

where $z \in \mathbb{C}$ is a complex number. One can show that the following identities hold true:

$$\begin{aligned} p_{\mathbf{a}}(z^k) &= p_{\uparrow_k \{\mathbf{a}\}}(z) \\ p_{\mathbf{a}}(z^k)p_{\mathbf{b}}(z^l) &= p_{\uparrow_k \{\mathbf{a}\} * \uparrow_l \{\mathbf{b}\}}(z) \\ p_{\mathbf{a}}(z)^d &= \underbrace{p_{(0, 0, \dots, 0, \mathbf{a})}(z)}_d \end{aligned}$$

for $d, k, l \in \mathbb{Z}^+$. If a sequence consists of zero elements between two non-zero elements, it is a non-contiguous sequence. Otherwise, it is a contiguous sequence.

The polynomial representation given in (1) corresponds to an OFDM symbol in continuous time if z is restricted to be on the unit circle in the complex plane, i.e., $z \in \{e^{j\frac{2\pi t}{T_s}} \mid 0 \leq t < T_s\}$, where T_s denotes the OFDM symbol duration. The instantaneous envelope power can be expressed as

$$|p_{\mathbf{a}}(z)|^2 = \rho_{\mathbf{a}}^+(0) + 2 \sum_{k=1}^{N-1} |\rho_{\mathbf{a}}^+(k)| \cos \left(\frac{2\pi t}{T_s} k + \angle \rho_{\mathbf{a}}(k) \right), \quad (2)$$

where $\rho_{\mathbf{a}}^+(k) = \sum_{i=0}^{N-k-1} a_i^* a_{i+k}$ is the aperiodic auto correlation (APAC) of the sequence \mathbf{a} for $k = 0, 1, \dots, N-1$ [17].

The instantaneous envelope power minimization of an OFDM symbol generated through a non-contiguous sequence in the frequency domain introduces more constraints as compared to the one with a contiguous sequence. For example, consider the interlace model given in Figure 1. If the same number of non-zero elements in an interlace is utilized contiguously in the frequency domain, the number of constraints that need to be met for 0 dB PAPR (i.e., $\rho_{\mathbf{a}}^+(k) = 0$ for $k \neq 0$) is $N_{\text{rb}}N_{\text{sc}} - 1$ based on (2). On the other hand, for $N_{\text{null}} \geq N_{\text{sc}}$, the number of constraints increases to $2N_{\text{rb}}N_{\text{sc}} - N_{\text{sc}} - N_{\text{rb}}$. As a numerical example, while the number of constraints for a contiguous resource allocation with 120 subcarriers is 119, the number of constraints for an interlace in LTE reaches to 218, which is more challenging to meet for a low PAPR design.

C. Complementary Sequences

The sequence pair (\mathbf{a}, \mathbf{b}) of length N is called a GCP if

$$\rho_{\mathbf{a}}(k) + \rho_{\mathbf{b}}(k) = 0, \quad \text{for } k \neq 0 \quad (3)$$

where the sequences \mathbf{a} and \mathbf{b} are CSs. By using the definition, one can show that the GCP (\mathbf{a}, \mathbf{b}) satisfies

$$|p_{\mathbf{a}}(z)|^2 + |p_{\mathbf{b}}(z)|^2 \Big|_{z=e^{j\frac{2\pi t}{T_s}}} = \underbrace{\rho_{\mathbf{a}}(0) + \rho_{\mathbf{b}}(0)}_{\text{constant}}. \quad (4)$$

The main property that we inherited from GCPs in this study is that the instantaneous peak power of the corresponding OFDM signal generated through a CS \mathbf{a} is bounded, i.e., $\max_t |p_{\mathbf{a}}(e^{j\frac{2\pi t}{T_s}})|^2 \leq \rho_{\mathbf{a}}(0) + \rho_{\mathbf{b}}(0)$. Therefore, based on (4), the PAPR of the OFDM signal is less than or equal to $10 \log_{10}(2) \approx 3$ dB if $\rho_{\mathbf{a}}(0) = \rho_{\mathbf{b}}(0)$ [20]. For the other interesting properties of GCPs, we refer the reader to the survey given in [21].

D. Unimodular Sequences

Let $\mathbf{x} = (x_0, x_1, \dots, x_{N-1}) \in \mathbb{C}^N$ be a sequence of length N . If $|x_i| = c$ for $i = 0, 1, \dots, N-1$, \mathbf{x} is referred to as a unimodular or constant-amplitude sequence of length N . Without loss of generality, we assume $c = 1$ in this study.

For a unimodular sequence \mathbf{x} , one can show that $\langle \mathbf{x} \odot \mathbf{s}_i, \mathbf{x} \odot \mathbf{s}_j \rangle = 0$ if $i \neq j$, where $\mathbf{s}_r = (e^{r\frac{2\pi i}{N} \times 0}, e^{r\frac{2\pi i}{N} \times 1}, \dots, e^{r\frac{2\pi i}{N} \times (N-1)})$ for $r = 0, 1, \dots, N-1$ [22]. Thus, $\{\mathbf{x} \odot \mathbf{s}_r \mid r = 0, 1, \dots, N-1\}$ is an orthogonal basis

where each sequence can be used in an OFDM transmitter with low-complexity operations, i.e., shifting the useful duration of OFDM signal generated through \mathbf{x} in time cyclically. For this reason, the unimodular sequences are suitable for code-domain orthogonal multiplexing in the uplink, which have been used for increasing the number of users or transmitting more information bits on the same time-frequency resources in both NR [18] and LTE uplink control channels [23].

E. Algebraic Representation of a Sequence

A generalized Boolean function is a function f that maps from $\mathbb{Z}_2^m = \{(x_1, x_2, \dots, x_m) \mid x_j \in \mathbb{Z}_2\}$ to \mathbb{Z}_H as $f : \mathbb{Z}_2^m \rightarrow \mathbb{Z}_H$ where H is an integer. We associate a sequence \mathbf{f} of length 2^m with the function $f(x_1, x_2, \dots, x_m)$ by listing its values as (x_1, x_2, \dots, x_m) ranges over its 2^m values in lexicographic order (i.e., the most significant bit is x_1). In other words, the $(x+1)$ th element of the sequence \mathbf{f} is equal to $f(x_1, x_2, \dots, x_m)$ where $x = \sum_{j=1}^m x_j 2^{m-j}$. Note that different generalized Boolean functions yield to different sequences as each generalized Boolean function can be uniquely expressed as a linear combination of the monomials over \mathbb{Z}_H [16]. For the sake of simplifying the notation, the sequence (x_1, x_2, \dots, x_m) and the function $f(x_1, x_2, \dots, x_m)$ are denoted by \mathbf{x} and $f(\mathbf{x})$, respectively.

III. THE PROPOSED SCHEMES

In this section, we first discuss two theorems, i.e., Theorem 1 and Theorem 2, to generate non-contiguous CSs. We then derive two schemes originating from Theorem 1 and Theorem 2. While the first scheme allows the users to transmit 1-2 bit information decodable by a non-coherent detector, the second scheme supports more than 2 bits by relying a generic CS encoder.

A. Fundamental Theorems

A theorem which generalizes Golay's concatenation and interleaving methods [15] can be restated as follows:

Theorem 1. Let (\mathbf{a}, \mathbf{b}) and (\mathbf{c}, \mathbf{d}) be GCPs of length N and M , respectively, and $\omega_1, \omega_2 \in \{u : u \in \mathbb{C}, |u| = 1\}$ and $k, l, d \in \mathbb{Z}$. Then, the sequences \mathbf{t} and \mathbf{r} where their polynomial representations are given by

$$p_{\mathbf{t}}(z) = \omega_1 p_{\mathbf{a}}(z^k) p_{\mathbf{c}}(z^l) + \omega_2 p_{\mathbf{b}}(z^k) p_{\mathbf{d}}(z^l) z^d, \quad (5)$$

$$p_{\mathbf{r}}(z) = \omega_1 p_{\mathbf{a}}(z^k) p_{\mathbf{d}}(z^l) - \omega_2 p_{\mathbf{b}}(z^k) p_{\mathbf{c}}(z^l) z^d, \quad (6)$$

construct a GCP.

Theorem 1 can be proved by using the GCP definition [9].

The special cases of Theorem 1 were discussed in earlier work for several purposes, e.g., binary contiguous CSs [21], [24] or multi-level contiguous CSs via \mathbf{c} and \mathbf{d} of length 1 [25]. In addition, Theorem 1 also plays a central role for generating non-contiguous CSs. For example, based on the identities given in Section II-B, z^d increases the degree of the polynomial $\omega_2 p_{\mathbf{b}}(z^k) p_{\mathbf{d}}(z^l)$ by d , which yields to two clusters in the sequence \mathbf{t} where the distance between them can be chosen arbitrarily. Similarly, $k > M$ or $l > N$ can

generate non-contiguous CS sequences due to the convolutions in each cluster. In Section III-B, we use Theorem 1 for transmitting 1 or 2 information bits to generate non-contiguous CSs compatible with an interlace with the careful choice of the parameters d , k , and l by starting from two different GCPs.

To support more information bits, it is important to generate many distinct CSs. However, Theorem 1 does not show how to generate distinct CSs. To address this issue, we propose the following theorem by utilizing an approach which extracts the algebraic structure of a recursion [17], as summarized in Appendix A:

Theorem 2 (Main Theorem). *Let $\pi = (\pi_n)_{n=1}^m$ and $\phi = (\phi_n)_{n=1}^m$ be sequences defined by permutations of $\{1, 2, \dots, m\}$. For any GCP $(\mathbf{c}_n, \mathbf{d}_n)$ of length $M_n \in \mathbb{Z}^+$, $U \in \mathbb{Z}_0^+$, $d_n \in \mathbb{Z}_0^+$, and $c_n, c', c'' \in [0, H)$ for $n = 1, 2, \dots, m$, let*

$$c_i(\mathbf{x}) = \frac{H}{2} \sum_{n=1}^{m-1} x_{\pi_n} x_{\pi_{n+1}} + \sum_{n=1}^m c_n x_{\pi_n}, \quad (7)$$

$$\begin{aligned} c_o(\mathbf{x}, z) = \prod_{n=1}^{m-1} p_{\mathbf{c}_{\phi_n}}(z) ((1 - x_{\pi_n})(1 - x_{\pi_{n+1}}))_2 \\ + p_{\mathbf{d}_{\phi_n}}(z) (x_{\pi_n}(1 - x_{\pi_{n+1}}))_2 \\ + p_{\tilde{\mathbf{d}}_{\phi_n}}(z) ((1 - x_{\pi_n})x_{\pi_{n+1}})_2 \\ + p_{\tilde{\mathbf{c}}_{\phi_n}}(z) (x_{\pi_n}x_{\pi_{n+1}})_2, \end{aligned} \quad (8)$$

where

$$f_i(\mathbf{x}) = c_i(\mathbf{x}) + c',$$

$$g_i(\mathbf{x}) = c_i(\mathbf{x}) + c'',$$

$$f_o(\mathbf{x}, z) = c_o(\mathbf{x}, z) (p_{\mathbf{c}_{\phi_m}}(z)(1 - x_{\pi_m})_2 + p_{\mathbf{d}_{\phi_m}}(z)x_{\pi_m}), \quad (9)$$

$$g_o(\mathbf{x}, z) = c_o(\mathbf{x}, z) (p_{\tilde{\mathbf{d}}_{\phi_m}}(z)(1 - x_{\pi_m})_2 + p_{\tilde{\mathbf{c}}_{\phi_m}}(z)x_{\pi_m}),$$

$$f_s(\mathbf{x}) = \sum_{n=1}^m d_n x_{\pi_n}.$$

Then, the sequences \mathbf{t} and \mathbf{r} where their polynomial representations are given by

$$p_{\mathbf{t}}(z) = \sum_{x=0}^{2^m-1} f_o(\mathbf{x}, z) \times \xi^{\text{if}_i(\mathbf{x})} \times z^{f_s(\mathbf{x})+xU}, \quad (10)$$

$$p_{\mathbf{r}}(z) = \sum_{x=0}^{2^m-1} g_o(\mathbf{x}, z) \times \xi^{\text{ig}_i(\mathbf{x})} \times z^{f_s(\mathbf{x})+xU} \quad (11)$$

construct a GCP, where $\xi = e^{\frac{2\pi}{H}}$.

The proof for Theorem 2 is given in Appendix B.

Theorem 2 captures the results in [16] and [17] while introducing new terms. For example, in Theorem 2, $f_i(\mathbf{x})$ and $g_i(\mathbf{x})$ are identical to the results given in [16] for $c_n, c', c'' \in \mathbb{Z}_H$ and [26] for $c_n, c', c'' \in \mathbb{Z}_H$, where $h \geq 1$ is an integer. It was shown that they yield to the codewords in the cosets of the first-order RM code within the second-order RM code. The function $f_s(\mathbf{x})$ in Theorem 2 is also proposed in [17] to generate non-contiguous CSs by increasing the degrees of the polynomials in the summands as in (10) and (11). On the other hand, $f_o(\mathbf{x}, z)$ and $g_o(\mathbf{x}, z)$ in [17] are different

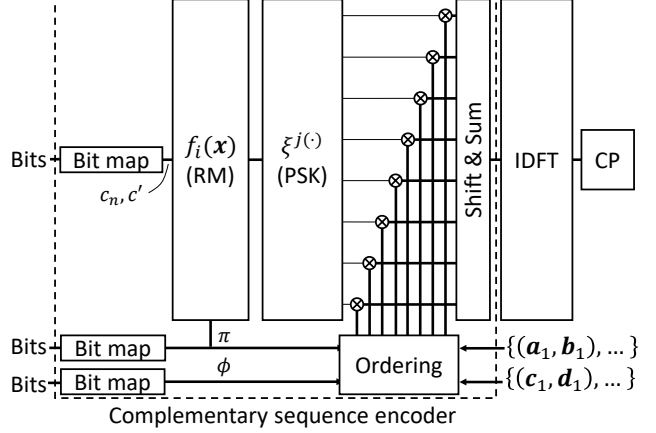


Figure 2. The complementary sequence encoder based on Theorem 2 for $m = 3$ and using it with an OFDM symbol.

from the ones in Theorem 2. While $f_o(\mathbf{x}, z)$ is equal to $g_o(\mathbf{x}, z)$ in [17], $f_o(\mathbf{x}, z)$ and $g_o(\mathbf{x}, z)$ are not identical in Theorem 2. In addition, $f_o(\mathbf{x}, z)$ and $g_o(\mathbf{x}, z)$ in Theorem 2 are the products of m polynomials where each polynomial in the product is either $p_{\mathbf{c}_{\phi_n}}(z)$, $p_{\mathbf{d}_{\phi_n}}(z)$, $p_{\tilde{\mathbf{d}}_{\phi_n}}(z)$, or $p_{\tilde{\mathbf{c}}_{\phi_n}}(z)$ for $n = 1, 2, \dots, m$. For example, let $m = 3$, $\pi = (3, 2, 1)$, and $\phi = (1, 2, 3)$. Then, x_{π_1} , x_{π_2} , and x_{π_3} can be listed as

$$\begin{bmatrix} 0 & 1 & 0 & 1 & 0 & 1 & 0 & 1 \\ 0 & 0 & 1 & 1 & 0 & 0 & 1 & 1 \\ 0 & 0 & 0 & 0 & 1 & 1 & 1 & 1 \end{bmatrix} \begin{aligned} x_{\pi_1} &= x_3 \\ x_{\pi_2} &= x_2 \\ x_{\pi_3} &= x_1 \end{aligned}.$$

By plugging ϕ , x_{π_1} , x_{π_2} , and x_{π_3} into (9), $f_o(\mathbf{x}, z)$ can be enumerated as

$$(f_o(\mathbf{x}, z))_{x=0}^{2^3-1} = (p_{\mathbf{c}_3}(z)p_{\mathbf{c}_2}(z)p_{\mathbf{c}_1}(z),$$

$$p_{\mathbf{c}_3}(z)p_{\mathbf{c}_2}(z)p_{\mathbf{d}_1}(z),$$

$$p_{\mathbf{c}_3}(z)p_{\mathbf{d}_2}(z)p_{\tilde{\mathbf{d}}_1}(z),$$

$$p_{\mathbf{c}_3}(z)p_{\mathbf{d}_2}(z)p_{\tilde{\mathbf{c}}_1}(z),$$

$$p_{\mathbf{d}_3}(z)p_{\tilde{\mathbf{d}}_2}(z)p_{\mathbf{c}_1}(z),$$

$$p_{\mathbf{d}_3}(z)p_{\tilde{\mathbf{d}}_2}(z)p_{\mathbf{d}_1}(z),$$

$$p_{\mathbf{d}_3}(z)p_{\tilde{\mathbf{c}}_2}(z)p_{\tilde{\mathbf{d}}_1}(z),$$

$$p_{\mathbf{d}_3}(z)p_{\tilde{\mathbf{c}}_2}(z)p_{\tilde{\mathbf{c}}_1}(z)). \quad (12)$$

On the other hand, the elements of $(f_o(\mathbf{x}, z))_{x=0}^{2^3-1}$ in [17] consist of only one polynomial.

Theorem 2 forms a generic CS encoder which supports a wide variety of sequence lengths and non-contiguous resource allocation. Consider the polynomial representation of \mathbf{t} given in (11). Since $f_o(\mathbf{x}, z)$ is the product of the m polynomials generated through the initial sequences, it is also equal to the polynomial representation of the convolutions of the corresponding sequences. Hence, for a given x , the resulting sequence length for $f_o(\mathbf{x}, z)$ is equal to $L = (\sum_{n=1}^m M_n) - m + 1$. The x th sequence is then multiplied with x th H -phase shift keying (PSK) symbol based on $f_i(\mathbf{x})$, as in (10). Since the degree of each polynomial is also increased by $z^{f_s(\mathbf{x})+xU}$, each phase-rotated sequence is padded by $f_s(\mathbf{x}) + xU$ zeros. The final sequence \mathbf{t} is then obtained by summing the 2^m shifted and phase-rotated sequences. The length of the final sequence can

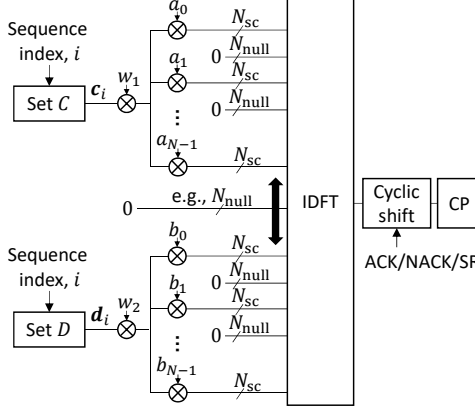


Figure 3. Transmitter structure for 1-2 bit transmission.

be calculated as $L + U(2^m - 1) + \sum_{n=1}^m d_n$. In Figure 2, we illustrate these steps for an OFDM transmitter where we configure the parameters π , ϕ , c_n , and c' based on information bits. In Section III-C, we utilize Theorem 2 to develop a scheme that can support more than 2 information bits in an LTE interlace while enabling orthogonal user multiplexing.

B. Scheme for 1-2 Bit Information

To be compatible with the interlace in Figure 1, we choose a GCP (\mathbf{a}, \mathbf{b}) of length $N_{\text{rb}}/2$ and a GCP $(\mathbf{c}_i, \mathbf{d}_i)$ of length N_{sc} where the elements of \mathbf{a} , \mathbf{b} , \mathbf{c} and \mathbf{d} are in the set $Q_1 \triangleq \{+, -, i, j\}$ for $i = 1, 2, \dots, K$. We then generate the interlace through (5) in Theorem 1 by setting $\mathbf{c} = \mathbf{c}_i$, $\mathbf{d} = \mathbf{d}_i$, $\omega_1 = \omega_2 = e^{\frac{i\pi}{4}}$, $k = N_{\text{sc}} + N_{\text{null}}$, $l = 1$, and $d = (N_{\text{sc}} + N_{\text{null}}) \times N_{\text{rb}}/2$.

In this scheme, \mathbf{a} and \mathbf{b} act as spreading sequences for the sequences \mathbf{c}_i and \mathbf{d}_i . This can be seen from the identities given in Section II-B as

$$p_{\mathbf{a}}(z^{N_{\text{sc}}+N_{\text{null}}})p_{\mathbf{c}}(z) = p_{\uparrow_{N_{\text{sc}}+N_{\text{null}}}\{\mathbf{a}\}*\mathbf{c}}(z), \quad (13)$$

and

$$p_{\mathbf{b}}(z^{N_{\text{sc}}+N_{\text{null}}})p_{\mathbf{d}}(z) = p_{\uparrow_{N_{\text{sc}}+N_{\text{null}}}\{\mathbf{b}\}*\mathbf{d}}(z). \quad (14)$$

In other words, the RBs are constructed with the phased rotated versions of \mathbf{c}_i and \mathbf{d}_i and the phase rotations are determined by the elements of \mathbf{a} and \mathbf{b} as shown in Figure 3. Based on the second part of (5) in Theorem 1, $d = (N_{\text{sc}} + N_{\text{null}}) \times N_{\text{rb}}/2$ null symbols are prepended to the sequence $\uparrow_{N_{\text{sc}}+N_{\text{null}}}\{\mathbf{b}\} * \mathbf{d}_i$. Hence, while the first half of the interlace is a function of \mathbf{a} and \mathbf{c}_i , the second part is generated through \mathbf{b} and \mathbf{d}_i as illustrated in Figure 1. By considering the interlace parameters in LTE eLAA and quadrature phase shift keying (QPSK) alphabet for the sequences, the interlace can be constructed with the proposed scheme via (5) when $k = 120$, $l = 1$, and $d = 600$ and the sequences \mathbf{a} , \mathbf{b} , \mathbf{c}_i , \mathbf{d}_i are chosen arbitrarily from the set provided from [27] as $\mathbf{a} = (+, +, +, j, i)$, $\mathbf{b} = (+, i, -, +, j)$, $\mathbf{c}_i = (+, +, +, +, -, -, +, i, j, -, +)$, and $\mathbf{d}_i = (+, +, i, i, +, +, -, +, +, -, +, -)$.

The proposed scheme offers flexibility for the interlace structure since N_{null} and d can be arbitrary integer numbers. For example, in one scenario, another user in the cell may need to transmit a random access signal by using a contiguous

allocation¹. To address this scenario, using a larger padding parameter d and a *single* pair of shorter spreading sequences \mathbf{a} and \mathbf{b} can generate the desired gap in the frequency; and the PAPR is still less than or equal to 3 dB for the same \mathbf{c}_i and \mathbf{d}_i . A similar strategy can be used for addressing the interlaces with different number of clusters due to the various bandwidth and subcarrier spacing configurations in NR-U.

1) *Reducing Cross-Correlation*: The proposed schemes simplifies the control channel design as it separates two complicated problems, i.e., the PAPR minimization under a non-contiguous resource allocation and low-cross correlation design of the sets for \mathbf{c}_i and \mathbf{d}_i to reduce potential interference scenarios (e.g., multi-access interference or inter-cell interference). For the first problem, as long as the sequences \mathbf{c}_i and \mathbf{d}_i for $i = 1, 2, \dots, K$ construct a GCP, the same spreading \mathbf{a} and \mathbf{b} can be utilized to limit the PAPR. For example, changing only the GCP (\mathbf{a}, \mathbf{b}) based on a different subcarrier spacing and bandwidth configuration in NR-U achieves to limit PAPR less than or equal to 3 dB without modifying the sequences in $C \triangleq \{\mathbf{c}_1, \mathbf{c}_2, \dots, \mathbf{c}_K\}$ and $D \triangleq \{\mathbf{d}_1, \mathbf{d}_2, \dots, \mathbf{d}_K\}$, that remarkably reduces the design complexity. For the second problem, the cross-correlation between any two sequences in C and D should be as low as possible to minimize the potential interference between the sequences. Due to the multipath channel, the signals may be exposed to additional shift in time within the cyclic prefix (CP). In this case, the cross-correlation should consider maximum peak cross correlation in time. In NR and LTE, the number of available base sequences is set to $K = 30$ for $N_{\text{sc}} = 12$. However, designing C and D such that $\langle \mathbf{c}_i, \mathbf{c}_j \odot \mathbf{s}_r \rangle \leq \beta$ and $\langle \mathbf{d}_i, \mathbf{d}_j \odot \mathbf{s}_r \rangle \leq \beta$ for $i \neq j$ and $i, j \in \{1, 2, \dots, K\}$, where $\mathbf{s}_r = (e^{r \frac{2\pi i}{N_{\text{sc}}} \times 0}, e^{r \frac{2\pi i}{N_{\text{sc}}} \times 1}, \dots, e^{r \frac{2\pi i}{N_{\text{sc}}} \times (N_{\text{sc}}-1)})$ and $r \in [0, N_{\text{sc}} - 1]$ is challenging task. Therefore, re-using the sets for different configurations is highly desirable. This naturally leads to the following question for the proposed scheme: Do there exist C and D for $K = 30$ and $N_{\text{sc}} = 12$, i.e., 30 different GCPs of length 12, such that the maximum correlation between any two sequences in each set for any non-integer r value is sufficiently small?

To answer this question, we consider a procedure which exploits the computer-generated GCPs provided in [27] for length 12 to obtain C and D . We initialize the algorithm with $I = 52$ GCPs of length 12 listed in [27] and populate as $S''_c = \{\mathbf{c}_1'', \dots, \mathbf{c}_I''\}$ and $S''_d = \{\mathbf{d}_1'', \dots, \mathbf{d}_I''\}$. For the i th seed GCP $(\mathbf{c}_i'', \mathbf{d}_i'')$, we first enumerate $J = 8$ equivalent GCPs by interchanging, reflecting both (i.e., reversing the order of the elements of the sequences), and conjugate reflecting original sequences in the seed GCP, which lead to the sets $S'_c = \{\mathbf{c}_1', \dots, \mathbf{c}_J'\}$ and $S'_d = \{\mathbf{d}_1', \dots, \mathbf{d}_J'\}$. Because of the properties of GCP, the $(\mathbf{c}_j', \mathbf{d}_j')$ still constructs GCPs for $j = 1, \dots, J$. For a given candidate GCP $(\mathbf{c}_j', \mathbf{d}_j')$, we calculate $\langle \mathbf{c}_i, \mathbf{c}_j' \odot \mathbf{s}_r \rangle$ and $\langle \mathbf{d}_i, \mathbf{d}_j' \odot \mathbf{s}_r \rangle$ for $\mathbf{c}_i \in C$ and $\mathbf{d}_i \in D$ and $r \in \{0, 1/Mu, \dots, (Mu-1)/Mu\}$ and $u > 1$. If the results are less than or equal to β for all r , we update C and D by

¹Contiguous allocation for random access signals typically improve the timing accuracy with a simple receiver due to the better auto-correlation properties.

Table I
THE SEQUENCES IN C AND D

i	c_i	d_i
1	(+, -, i, j, +, -, -, +, +, +, +)	(-, +, -, +, +, -, +, +, j, j, +, +)
2	(+, -, j, i, +, -, -, +, +, +, +)	(-, +, -, +, +, +, +, +, i, i, +, +)
3	(+, +, +, i, +, -, j, +, -, +, +)	(+, +, -, -, i, +, +, +, +, -, +, -)
4	(+, -, +, i, +, j, +, +, +, +)	(-, +, -, +, j, +, +, j, -, +, +)
5	(+, +, +, j, +, +, +, +, +, +)	(+, +, -, +, j, +, +, j, +, +, +, -)
6	(+, -, +, j, +, +, +, +, +, +)	(-, +, -, +, i, +, +, +, i, -, +, +)
7	(+, +, +, i, +, +, j, +, -, +, +)	(+, +, -, +, i, -, -, i, +, +, +)
8	(+, -, +, i, +, j, +, +, +, +)	(-, +, -, +, j, +, -, j, -, +, +)
9	(+, +, +, j, +, +, +, +, +, +)	(+, +, -, +, j, +, +, +, +, +, +)
10	(+, -, +, j, +, +, +, +, +, +)	(-, +, -, +, i, +, +, +, +, +, +)
11	(+, +, -, +, j, +, +, +, +, +)	(-, +, -, +, j, +, +, +, +, +, +)
12	(+, +, +, +, i, +, +, +, +, +)	(-, +, +, +, i, +, +, +, +, +, +)
13	(+, +, +, +, i, +, j, +, +, +, +)	(+, +, +, +, j, +, +, +, +, +, +)
14	(+, +, +, +, j, +, +, +, +, +)	(+, +, +, +, i, +, +, +, +, +, +)
15	(+, +, +, +, j, +, +, +, +, +)	(-, +, +, +, j, +, +, +, +, +, +)
16	(+, +, +, +, i, +, +, +, +, +)	(-, +, +, +, i, +, +, +, +, +, +)
17	(+, +, +, +, i, +, +, j, +, +, +)	(+, +, +, +, j, +, +, +, +, +, +)
18	(+, +, +, +, j, +, +, +, +, +)	(+, +, +, +, i, +, +, +, +, +, +)
19	(+, +, +, +, i, +, +, +, +, +)	(+, +, +, +, +, +, j, +, +, +, +)
20	(+, +, +, +, +, j, j, +, +, +, +)	(-, +, +, +, j, +, +, +, +, +, +)
21	(+, +, +, +, j, j, +, +, +, +, +)	(+, +, +, +, +, +, i, j, +, +, +, +)
22	(+, +, +, +, +, i, +, +, +, +, +)	(-, +, +, +, i, +, +, +, +, +, +)
23	(+, +, +, +, +, +, +, +, +, +, +)	(+, +, +, +, +, +, +, +, +, +, +)
24	(+, +, +, +, +, +, +, +, +, +, +)	(+, +, +, +, +, +, +, +, +, +, +)
25	(+, +, +, +, +, +, +, +, +, +, +)	(+, +, +, +, +, +, +, +, +, +, +)
26	(+, +, +, +, +, +, +, +, +, +, +)	(-, +, +, +, +, +, +, +, +, +, +)
27	(+, +, +, +, +, i, j, +, +, +, +)	(+, +, +, +, i, +, +, +, +, +, +)
28	(+, +, +, +, i, j, +, +, +, +, +)	(-, +, +, +, +, +, j, +, +, +, +)
29	(+, +, +, +, i, +, +, +, +, +, +)	(+, +, +, +, i, +, +, +, +, +, +)
30	(+, +, +, +, j, +, +, +, +, +, +)	(-, +, +, +, i, +, +, +, +, +, +)

including the sequences in the candidate GCP to the sets.

We list the sets obtained for c_i and d_i in Table I for $\beta = 0.715$ and $u = 128$. Based on the aforementioned procedure, we could not obtain C and D when $\beta < 0.715$ for $K = 30$ and $N_{\text{sc}} = 12$. However, the numerical results given in Section IV show that the maximum cross-correlation is still less than the ones for Zadoff-Chu (ZC) sequences and the sequences adopted in NR [18]. It is also worth noting that the sets obtained for c_i and d_i are not unique and are based on the initial seed sequences.

2) *User-multiplexing*: The proposed scheme is based on unimodular sequences for each RB in an interlace. When the unimodular sequences are employed on each RB, the number of orthogonal resources generated through cyclic-shifts in time is equal to the size of RBs although the interlace has $N_{\text{sc}}N_{\text{rb}}$ non-zero elements. For example, if there are $N_{\text{rb}} = 10$ RBs in one interlace and each RB consists of $N_{\text{sc}} = 12$ subcarriers, there are 12 orthogonal resources generated through the shifts in *time*. 12 resources can be shared by 6 users to transmit 1-bit information (e.g., ACK/NACK) or 3 users to transmit 2-bit information (e.g., ACK/NACK and scheduling request). The receiver can detect the corresponding sequences in each RB to decode the information.

C. Scheme for More Than 2 Bit Information

In LTE and NR, N_{sc} is fixed to $2^3 \times 3 = 12$ subcarriers. For this reason, we set $m = 3$ which leads to $2^3 H$ -PSK symbols and choose two initial sequences in Theorem 2 based on length 3 and length $N_{\text{rb}}/2$. Let (\mathbf{a}, \mathbf{b}) be a GCP of length 3, and (\mathbf{c}, \mathbf{d}) be a GCP of length $N_{\text{rb}}/2$. The following configurations result in CSs compatible with the interlace in Figure 1:

- Configuration 1: $(\mathbf{c}_1, \mathbf{d}_1) = ((+), (+))$, $(\mathbf{c}_2, \mathbf{d}_2) = (\mathbf{a}, \mathbf{b})$, $(\mathbf{c}_3, \mathbf{d}_3) = (\uparrow_{2(N_{\text{null}}+N_{\text{sc}})} \{\mathbf{c}\}, \uparrow_{2(N_{\text{null}}+N_{\text{sc}})} \{\mathbf{d}\})$, $U = 3$, $d_{\pi_n=1} = N_{\text{null}} + N_{\text{sc}} - 4U$, and $d_{\pi_n \neq 1} = 0$
- Configuration 2: $(\mathbf{c}_1, \mathbf{d}_1) = ((+), (+))$, $(\mathbf{c}_2, \mathbf{d}_2) = (\mathbf{a}, \mathbf{b})$, $(\mathbf{c}_3, \mathbf{d}_3) = (\uparrow_{N_{\text{null}}+N_{\text{sc}}} \{\mathbf{c}\}, \uparrow_{N_{\text{null}}+N_{\text{sc}}} \{\mathbf{d}\})$, $U = 3$, $d_{\pi_n=1} = (N_{\text{null}} + N_{\text{sc}})N_{\text{rb}}/2 - 4U$, and $d_{\pi_n \neq 1} = 0$
- Configuration 3: $(\mathbf{c}_1, \mathbf{d}_1) = ((+), (+))$, $(\mathbf{c}_2, \mathbf{d}_2) = (\uparrow_4 \{\mathbf{a}\}, \uparrow_4 \{\mathbf{b}\})$, $(\mathbf{c}_3, \mathbf{d}_3) = (\uparrow_{2(N_{\text{null}}+N_{\text{sc}})} \{\mathbf{c}\}, \uparrow_{2(N_{\text{null}}+N_{\text{sc}})} \{\mathbf{d}\})$, $U = 1$, $d_{\pi_n=1} = N_{\text{null}} + N_{\text{sc}} - 4U$, and $d_{\pi_n \neq 1} = 0$
- Configuration 4: $(\mathbf{c}_1, \mathbf{d}_1) = ((+), (+))$, $(\mathbf{c}_2, \mathbf{d}_2) = (\uparrow_4 \{\mathbf{a}\}, \uparrow_4 \{\mathbf{b}\})$, $(\mathbf{c}_3, \mathbf{d}_3) = (\uparrow_{N_{\text{null}}+N_{\text{sc}}} \{\mathbf{c}\}, \uparrow_{N_{\text{null}}+N_{\text{sc}}} \{\mathbf{d}\})$, $U = 1$, $d_{\pi_n=1} = (N_{\text{null}} + N_{\text{sc}})N_{\text{rb}}/2 - 4U$, and $d_{\pi_n \neq 1} = 0$

While Configuration 1 and Configuration 2 cascade the modulated and spread sequences \mathbf{a} , \mathbf{b} , $\tilde{\mathbf{a}}$, and $\tilde{\mathbf{b}}$ in each RB, Configuration 3 and Configuration 4 interleave the elements of these sequences. The difference between Configuration 1 and Configuration 2 is that they shuffle the sequences in RBs in the interlace in a different order because of the choices of up-sampling factors and $d_{\pi_n=1}$. Similarly, Configuration 3 and Configuration 4 yields to the different orders in the interlace. For all configurations, N_{null} and N_{rb} can chosen flexibly without concern of increasing the PAPR, which addresses various potential subcarrier spacing and bandwidth configurations in NR-U with a single design.

Each configuration leads to $(m!)^2 H^{m+1}$ CSs compatible with the interlace structure in LTE due to the $m!$ permutations of π and ϕ , and H different values for $c_{n=1,2,\dots,m}$ and c' , which gives 9216 CSs with a QPSK alphabet for $m = 3$. Therefore, $\lfloor \log_2 9216 \rfloor = 13$ information bits can be transmitted for each configuration. The number of generated CSs can be increased by modifying (\mathbf{a}, \mathbf{b}) and (\mathbf{c}, \mathbf{d}) . For example, interchanging the sequences in a GCP, i.e., (\mathbf{b}, \mathbf{a}) , or conjugate reflecting one of the sequences in a GCP, e.g., $(\tilde{\mathbf{c}}, \mathbf{d})$, also lead to GCPs [27]. Hence, it is possible to generate 64 different (\mathbf{a}, \mathbf{b}) and (\mathbf{c}, \mathbf{d}) combinations. As a result, overall, there exist at least $64 \times 4 \times 9216 = 2359296$ CSs, which can be mapped to the maximum 21 information bits. Note that the rotating the phase of the GCP, e.g., $(\omega_1 \times \mathbf{a}, \omega_2 \times \mathbf{b})$, does not yield different complementary sequences as the impact of the rotations on (21) can be reduced to (7) [17].

1) *User-Multiplexing*: To allow orthogonal user-multiplexing within the interlace while enabling a low-complexity receiver, the sequences in each RB from different users may need to be orthogonal to each other. To meet this condition, we exploit the property of the unimodular sequences discussed in Section II-D and consider only of the configurations, e.g., Configuration 1. We obtain three orthogonal resources within each RB by modulating unimodular \mathbf{a} and \mathbf{b} as $\mathbf{a} \odot \mathbf{s}_r$ and $\mathbf{b} \odot \mathbf{s}_r$, respectively, where $\mathbf{s}_r = (e^{r \frac{2\pi i}{3} \times 0}, e^{r \frac{2\pi i}{3} \times 1}, e^{\frac{r 2\pi i}{3} \times 2})$ and $r \in \{0, 1, 2\}$. In addition, to maintain the orthogonality within each RB, we fix the locations of $\mathbf{a} \odot \mathbf{s}_r$ and $\mathbf{b} \odot \mathbf{s}_r$ on each RB. One way of achieving it is to set $\phi_{m=3} = 2$ and $\pi_{m=3} = 1$, which result in $\pi \in \{(3, 2, 1), (2, 3, 1)\}$ and $\phi \in \{(3, 1, 2), (1, 3, 2)\}$. The rationale behind this choice can be understood by expressing

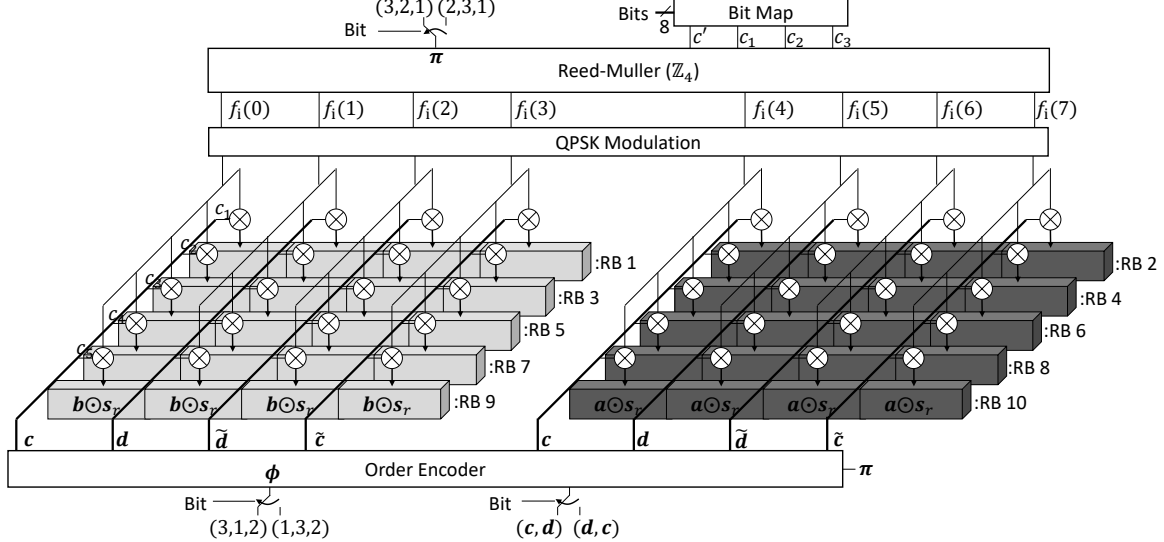


Figure 4. The location of \mathbf{a} and \mathbf{b} on each RB for Configuration 1. The phases of \mathbf{a} and \mathbf{b} are modified based on the order encoder and the RM code.

(9) for $\phi_{m=3} = 2$ and $\pi_{m=3} = 1$ as

$$f_o(\mathbf{x}, z) = c_o(\mathbf{x}, z)(p_{\mathbf{a} \odot \mathbf{s}}(z)(1 - x_1)_2 + p_{\mathbf{b} \odot \mathbf{s}}(z)x_1). \quad (15)$$

While $c_o(\mathbf{x}, z)$ takes different values depending on \mathbf{c} , \mathbf{d} , and the first two elements of π and ϕ , the remaining term in (15) places $\mathbf{a} \odot \mathbf{s}$ and $\mathbf{b} \odot \mathbf{s}_r$ in a fixed order. Therefore, the sequences $\mathbf{a} \odot \mathbf{s}_r$ and $\mathbf{b} \odot \mathbf{s}_r$ are multiplied with the elements of \mathbf{c} , \mathbf{d} , $\tilde{\mathbf{c}}$, and $\tilde{\mathbf{d}}$ and the outcome of $f_i(\mathbf{x})$ and mapped to the fixed subcarriers locations.

The proposed scheme enables three users to transmit $\log_2(2^2 H^{m+1}) = 10$ bits on the same interlace for a given GCP (\mathbf{c}, \mathbf{d}) . The number of bits can be increased if the initial sequences \mathbf{c} and \mathbf{d} are modified. For example, if the sequences in (\mathbf{c}, \mathbf{d}) are interchanged, the number of bits can be increased to 11 bits. Note that modifying \mathbf{c} and \mathbf{d} does not destroy the orthogonality between the sequences from different users as $\mathbf{a} \odot \mathbf{s}_r$ and $\mathbf{b} \odot \mathbf{s}_r$ are multiplied with scalars depending on the elements of \mathbf{c} , \mathbf{d} , $\tilde{\mathbf{c}}$, and $\tilde{\mathbf{d}}$. However, it requires an estimation of the modification at the receiver side.

In Figure 4, we illustrate how \mathbf{a} and \mathbf{b} are placed in each RB and modified based on $f_i(\mathbf{x})$ and $f_o(\mathbf{x}, z)$ for $N_{\text{rb}} = 10$. Interchanging \mathbf{a} and \mathbf{b} , the values of π and ϕ are controlled with 3 information bits. The output of the order encoder is exemplified for $\pi = (3, 2, 1)$ and $\phi = (3, 1, 2)$, which gives $(\mathbf{c}, \mathbf{d}, \tilde{\mathbf{d}}, \tilde{\mathbf{c}}, \mathbf{c}, \mathbf{d}, \tilde{\mathbf{d}}, \tilde{\mathbf{c}})$. The parameters $c_{n=1,2,3}, c' \in \mathbb{Z}_4$ are set based on 8 information bits. The bit mapping can be done based on Gray mapping, e.g., $00 \rightarrow 0, 01 \rightarrow 1, 10 \rightarrow 3$, and $11 \rightarrow 2$, to improve the error rate performance. Since the output of the generalized RM code are distributed to 5 different RBs as in Figure 4, the proposed scheme inherently exploits the frequency diversity in the frequency selective channels.

2) *Receiver Design:* The proposed scheme is compatible with the RM code in [16]. Thus, a simple receiver can be developed by re-using the minimum-likelihood decoder proposed in [28] for first-order RM codes. For our approach, we first separate the users by using the orthogonality among users, which lead to 4 complex values for each RB. We

then coherently combine $N_{\text{rb}}/2$ complex values distributed to $N_{\text{rb}}/2$ different RBs based on the minimum mean square error (MMSE) criterion. Subsequently, we use the minimum-distance decoder in [28] to obtain $c_{n=1,2,3}$ and c' . We perform this operation for 8 different hypotheses due to the combinations of interchange of \mathbf{a} and \mathbf{b} , and the values of π and ϕ . We choose the best hypothesis based on the minimum distance criterion. Our receiver introduces $N_{\text{rb}}N_{\text{sc}} + 8 \times N_{\text{rb}}N_{\text{sc}}/3$ complex multiplications and $2/3N_{\text{rb}}N_{\text{sc}} + 8 \times 8(N_{\text{rb}}/2 - 1)$ complex summations for the user separation and the hypothesis testing over the complexity of the maximum-likelihood (ML) decoder which is low for $m = 3$ as reported in [28].

IV. NUMERICAL ANALYSIS

In this section, we compare the proposed schemes with various potential schemes numerically based on LTE eLAA interlace parameters. For the proposed scheme for 1-2 bits, we employ the sequences given in Table I and the spreading sequences as $\mathbf{a} = (+, +, +, j, i)$, $\mathbf{b} = (+, i, -, +, j)$. For comparison, we consider NR sequences [18] on each RB in the interlace by introducing three PAPR minimization techniques. The first two methods rely on the optimal phase rotation with the QPSK alphabet for each RB for a given sequence, i.e., PTS approach, which prioritize either cubic metric (CM) or PAPR. The third approach applies a modulation operation to the sequence on each RB as a function of the occupied RB index [29]. In other words, the sequence on k th occupied RB in the interlace is multiplied with the sequence $(e^{j\frac{2\pi i}{N_{\text{sc}}} \times 0}, e^{j\frac{2\pi i}{N_{\text{sc}}} \times 1}, \dots, e^{j\frac{2\pi i}{N_{\text{sc}}} \times (N_{\text{sc}}-1)})$ for $k = 0, 1, \dots, 9$. We refer to this operation as *cycling* since the signal component located on each RB is cyclically shifted in time. For the fourth design, we generate all possible ZC sequences of length 113 (cyclic padded to 120) and select the best 30 sequences based on the PAPR of the corresponding signals after they are mapped to the interlace. At the receiver side, we use an energy detector based on Neyman-Pearson lemma. We first detect the

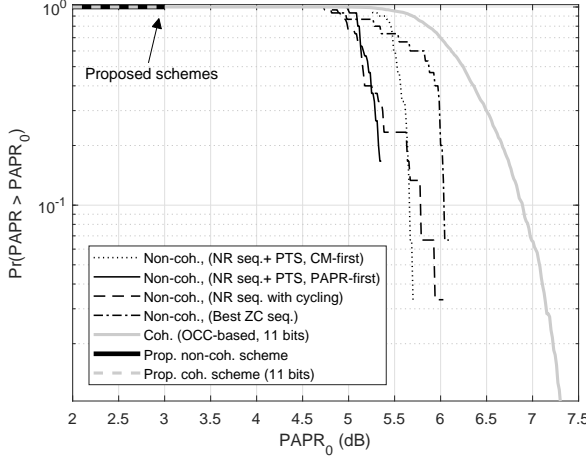


Figure 5. PAPR performance.

energy on the resources. If there is energy, we determine if it is ACK sequence or NACK sequence.

For more than 2 bits, we consider the scheme discussed in Section III-C1 and set $\mathbf{a} = (+, i, +)$, $\mathbf{b} = (+, +, -)$, $\mathbf{c} = (+, +, +, j, i)$, and $\mathbf{d} = (+, i, -, +, j)$. We compare it with an approach which uses different DFT-based orthogonal cover codes (OCCs) on each RB [3]. For this scheme, we consider (20,11) linear block code in LTE [23] and map the coded bits to 10 QPSK symbols. To reduce the PAPR, each QPSK symbol is multiplied with a distinct column of a DFT matrix (i.e., OCC) and the resulting columns vectors mapped to the 10 RBs of the interlace. At the receiver side, after the received signal is processed with an MMSE equalizer, a minimum distance decoder is utilized to receive the information bits.

A. PAPR/CM Results

In Figure 5, the PAPR distribution for all schemes are provided. For the alternative non-coherent schemes, the optimal spreading sequences prioritize PAPR or CM yield to a maximum PAPR of 5.3 dB and 5.7 dB, respectively, while the ZC sequences limits the PAPR to 6 dB. The cycling reduces the maximum PAPR to 5.9 dB. The PAPR for the coherent scheme in [3] for more than 2 bits reaches to 7.2 dB. On the other hand, the proposed schemes offer substantially improved PAPR results and limit the PAPR to 3 dB as they exploit CSs. The improvements in terms of PAPR is the range of 2.7-3 dB and 4.2 dB as compared to alternative non-coherent and coherent schemes, respectively.

Another metric that characterizes the fluctuation of the resulting signal is the CM. We calculate the CM in dB as $CM = 20 \log_{10}(\text{rms}\{v_{\text{norm}}^3(t)\})/1.56$, where $v_{\text{norm}}(t)$ is the synthesized signal in time with the power of 1 [30]. In Figure 6, we compare the CM distributions for the aforementioned schemes. Similar to the PAPR results, the proposed schemes improve the CM within the range of 0.8-1.8 dB as compared to the alternative approaches.

B. Cross-correlation Performance

We evaluate the cross-correlation performance of sequence designed for the non-coherent scheme by calculating $\rho =$

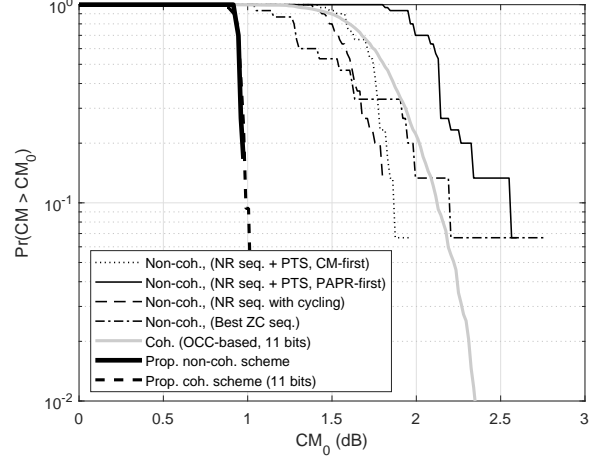


Figure 6. CM performance.

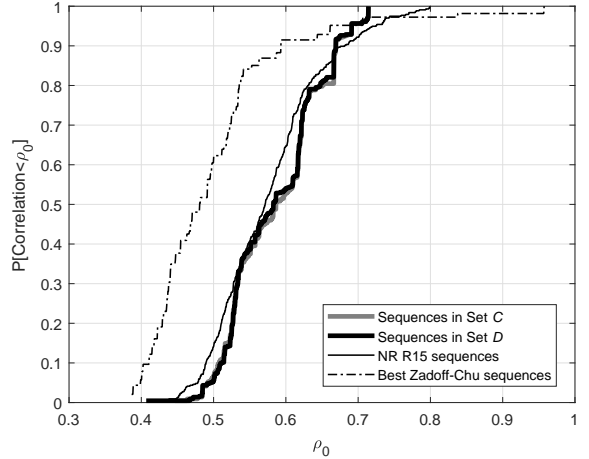


Figure 7. Cross-correlation results.

$\max\{|\text{IDFT}\{\mathbf{x}_i \odot \mathbf{x}_j^*\}, N_{\text{IDFT}}\}|\}/N_{\text{sc}}$, where \mathbf{x}_i is the i th sequence in the set, $i \neq j$ and $\text{IDFT}\{\cdot, N_{\text{IDFT}}\}$ is the unnormalized DFT operation of size N_{IDFT} [30]. To achieve a large oversampling in time, we choose $N_{\text{IDFT}} = 4096$. In Figure 7, we provide the distribution of ρ for different schemes. The ZC sequences fails as the maximum cross-correlation reaches up to 0.95 although 50 percentile performance is better than the other methods. The set of NR sequences causes to 0.8 for the maximum correlation. On the other hand, the maximum correlations for the both sets C and D are 0.715 as we set $\beta = 0.715$. Hence, the proposed non-coherent scheme provides robustness against potential interference between the sequences by minimizing the maximum cross-correlation and superior to NR sequences.

C. False Alarm and Miss Detection Results

In this section, we demonstrate the impact of interlacing on the ACK-to-NACK rate and the ACK miss-detection rate for a given DTX-to-ACK probability, as compared to the single-RB approach. The DTX-to-ACK and NACK-to-ACK rates correspond to the probability of ACK detection when there is no signal or a NACK is being transmitted, respectively. The

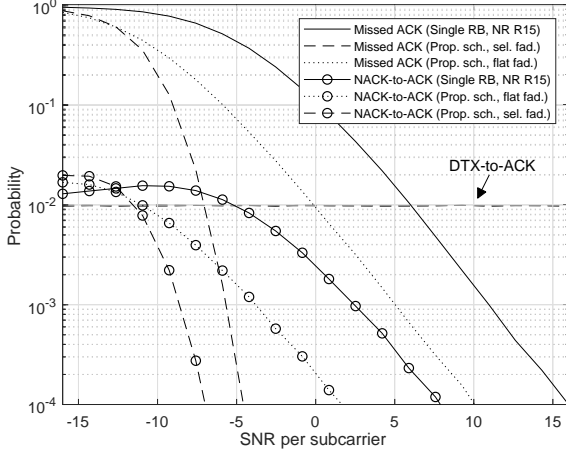


Figure 8. Receiver performance for the proposed scheme for 2 bits.

ACK miss detection rate is the probability of not detecting ACK when ACK is actually being transmitted. For the single-RB approach, we consider NR uplink control channel Format 0. To show the limits, we consider two extreme channel conditions where the occupied RBs in an interlace experience the same fading coefficients, i.e., flat fading, or independent-and-identically distributed (i.i.d.) Rayleigh fading coefficients to model selective fading. In practice, there is always correlation between channel coefficients. However, the correlation can decrease significantly for a large spacing between the occupied RBs in an interlace.

In the simulations, we set DTX-to-ACK probability to 1% and consider 2 receive antennas. We provide curves based on signal-to-noise ratio (SNR) per subcarrier as it reveals the benefit of interlace under the PSD requirement in the unlicensed band as compared to single RB transmission. The results in Figure 8 show that the interlace yields significantly improved performance as compared the single-RB approach due to the increased signal power under the PSD requirement. When the channel is frequency-selective, the slopes of the NACK-to-ACK and ACK miss-detection rates change remarkable as the non-contiguous resource allocation exploits the frequency diversity.

D. BLER Performance

In Figure 9, we compare the block-error rate (BLER) performance of the proposed scheme and the scheme in [3] for 11 bits transmission and 2 receive antennas. While the performance differences between two schemes are negligible for additive white Gaussian noise (AWGN) and flat fading channels, the proposed scheme is 1-2 dB better than the one in [3]. The performance difference is because the receiver for the proposed scheme coherently combine the symbols on different RBs before the ML detector whereas the receiver for the scheme in [3] cannot exploit selectivity without a high-complexity receiver as the modulation symbols are not spread to different RBs in this scheme. It is also worth noting that the proposed scheme also offers extra PAPR and CM gains, which are about 4.2 dB and 1.3 dB, respectively, as compared to the scheme in [3].

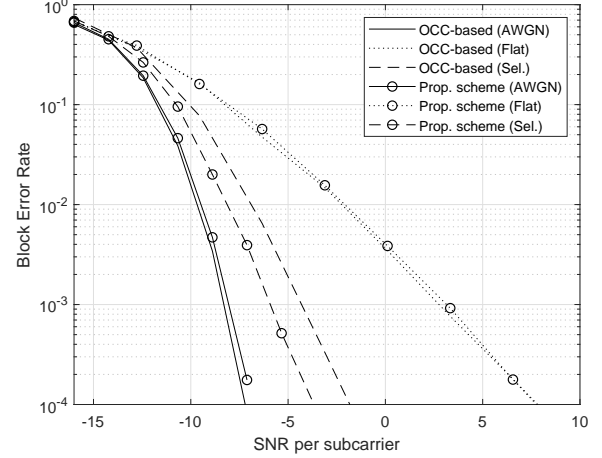


Figure 9. BLER comparison of the proposed scheme and OCC-based scheme in [3] for 11 bits.

V. CONCLUDING REMARKS

In this study, we propose two schemes for uplink control channels which consist of non-contiguous RBs in the frequency by exploiting GCPs via Theorem 1 and Theorem 2. The main benefit of the proposed schemes is that they address the PAPR problem of OFDM signals while allowing a flexible non-contiguous resource allocation for an interlace. For example, the number of null symbols between the RBs or the number of RBs in an interlace can be chosen flexibly with minor modifications in both proposed schemes. In all cases, the PAPR of the corresponding signal is less than or equal to 3 dB. With comprehensive numerical analysis, we show that the PAPR gain is around 3–4 dB as compared other schemes considered in this study.

The first scheme can be considered as an extension of the uplink control channel Format 0 in NR for 1-2 bit transmission in an unlicensed spectrum. It separates the PAPR minimization and low-cross correlation problems. While the first challenge is solved by choosing the sequences for RBs as a GCP in the light of Theorem 1, the second problem is addressed by design a set of GCPs for RBs. For the second scheme, we develop a new theorem, i.e., Theorem 2, which can be used to create a generic CS encoder that is capable of generating a wide-variety of CSs. By exploiting generalized Boolean functions and the combination of the initial sequence, we show that it is possible to transmit at least 21 bits in an LTE interlace while keeping the PAPR less than or equal to 3 dB. With numerical analysis, we also show the same scheme allows 3 users to transmit 11 bits on the same interlace while providing 1.5 dB SNR gain in frequency-selective channels and 4.2 dB PAPR gain.

APPENDIX A ALGEBRAIC STRUCTURE OF A RECURSION

For $n = 1, 2, \dots, m$, consider a recursion given by

$$\begin{aligned} p^{(n)} &= \mathcal{O}_{11}^{(n)}(p^{(n-1)}) + \mathcal{O}_{12}^{(n)}(q^{(n-1)})w^{2^{\psi_n}}, \\ q^{(n)} &= \mathcal{O}_{21}^{(n)}(p^{(n-1)}) + \mathcal{O}_{22}^{(n)}(q^{(n-1)})w^{2^{\psi_n}}, \end{aligned} \quad (16)$$

where w is an arbitrary complex number, ψ_n is the n th element of the sequence $\psi \triangleq (\psi_n)_{i=1}^m$ defined by the permutation of $\{0, 1, \dots, m-1\}$, $\mathcal{O}_{ij}^{(n)} \in \{O_0^{(n)}, O_1^{(n)}\}$ is a linear operator which transforms one function to another function in \mathcal{F} , and $p^{(0)} = q^{(0)} = r$. In [17], it has been shown that $p^{(m)}$ and $q^{(m)}$ can be obtained as

$$p^{(m)} = \sum_{x=0}^{2^m-1} \overbrace{O_{f_m(x)}^{(m)} \dots O_{f_n(x)}^{(n)} \dots O_{f_2(x)}^{(2)} O_{f_1(x)}^{(1)}(r)}^{F_x(r)} w^x, \quad (17)$$

and

$$q^{(m)} = \sum_{x=0}^{2^m-1} \overbrace{O_{g_m(x)}^{(m)} \dots O_{g_n(x)}^{(n)} \dots O_{g_2(x)}^{(2)} O_{g_1(x)}^{(1)}(r)}^{G_x(r)} w^x, \quad (18)$$

where

$$f_n(\mathbf{x}) = \begin{cases} b_{11}^{(n)}(1 - x_{\pi_n}) + b_{12}^{(n)}x_{\pi_n} & n = m \\ b_{11}^{(n)}(1 - x_{\pi_n})(1 - x_{\pi_{n+1}}) \\ + b_{12}^{(n)}x_{\pi_n}(1 - x_{\pi_{n+1}}) \\ + b_{21}^{(n)}(1 - x_{\pi_n})x_{\pi_{n+1}} \\ + b_{22}^{(n)}x_{\pi_n}x_{\pi_{n+1}} & n < m \end{cases}, \quad (19)$$

$$g_n(\mathbf{x}) = \begin{cases} b_{21}^{(n)}(1 - x_{\pi_n}) + b_{22}^{(n)}x_{\pi_n} & n = m \\ b_{11}^{(n)}(1 - x_{\pi_n})(1 - x_{\pi_{n+1}}) \\ + b_{12}^{(n)}x_{\pi_n}(1 - x_{\pi_{n+1}}) \\ + b_{21}^{(n)}(1 - x_{\pi_n})x_{\pi_{n+1}} \\ + b_{22}^{(n)}x_{\pi_n}x_{\pi_{n+1}} & n < m \end{cases}, \quad (20)$$

for $n = 1, 2, \dots, m$, where $\pi_n = m - \psi_n$ is the n th element of the sequence $\pi \triangleq (\pi_n)_{n=1}^m$, $b_{ij}^{(n)} = 0$ if $\mathcal{O}_{ij}^{(n)} = O_0^{(n)}$ and $b_{ij}^{(n)} = 1$ if $\mathcal{O}_{ij}^{(n)} = O_1^{(n)}$. The vector $[b_{11}^{(n)} \ b_{12}^{(n)} \ b_{21}^{(n)} \ b_{22}^{(n)}]$ denotes the configuration vector \mathbf{b}_n .

The Boolean functions $f_n(\mathbf{x})$ and $g_n(\mathbf{x})$ show which of the two operators, i.e., $O_0^{(n)}$ and $O_1^{(n)}$, are involved in the construction of $F_x(r)$ and $G_x(r)$ by setting the indices as $O_{f_n(x)}$ and $O_{g_n(x)}$, respectively. The binary sequences associated with $f_n(\mathbf{x})$ and $g_n(\mathbf{x})$ are referred to as the n th construction sequences of $p^{(m)}$ and $q^{(m)}$ for $n = 1, 2, \dots, m$.

APPENDIX B

PROOF OF THEOREM 2

Proof. By using Theorem 1, a recursion which generates a GCP $(\mathbf{a}^{(m)}, \mathbf{b}^{(m)})$ for $m \geq 1$ can be given by

$$\begin{aligned} p_{\mathbf{a}^{(n)}}(z) &= p_{\mathbf{c}_n}(z)p_{\mathbf{a}^{(n-1)}}(z) + \omega_n p_{\mathbf{d}_n}(z)p_{\mathbf{b}^{(n-1)}}(z)z^{d_n}w^{2^{\psi_n}}, \\ p_{\mathbf{b}^{(n)}}(z) &= p_{\tilde{\mathbf{d}}_n}(z)p_{\mathbf{a}^{(n-1)}}(z) - \omega_n p_{\tilde{\mathbf{c}}_n}(z)p_{\mathbf{b}^{(n-1)}}(z)z^{d_n}w^{2^{\psi_n}}, \end{aligned} \quad (21)$$

where $\mathbf{a}^{(0)} = \mathbf{b}^{(0)} = 1$, $(\mathbf{c}_n, \mathbf{d}_n)$ is the n th GCP of length $M_n \in \mathbb{Z}^+$, $\omega_n, w \in \{u : u \in \mathbb{C}, |u| = 1\}$ are arbitrary complex numbers of unit magnitude, $d_n \in \mathbb{Z}$ for $n = 1, 2, \dots, m$, and ψ_n is the n th element of the sequence $\psi = (\psi_n)_{i=1}^m$

defined by the permutation of $\{0, 1, \dots, m-1\}$. The recursion in (21) can be re-expressed as

$$\begin{aligned} p^{(n)} &= C_1^{(n)} D_0^{(n)} \tilde{C}_0^{(n)} \tilde{D}_0^{(n)} \Delta_0^{(n)} \Omega_0^{(n)} S_0^{(n)}(p^{(n-1)}) \\ &\quad + C_0^{(n)} D_1^{(n)} \tilde{C}_1^{(n)} \tilde{D}_0^{(n)} \Delta_1^{(n)} \Omega_1^{(n)} S_0^{(n)}(q^{(n-1)}) w^{2^{\psi_n}}, \\ q^{(n)} &= C_0^{(n)} D_0^{(n)} \tilde{C}_0^{(n)} \tilde{D}_1^{(n)} \Delta_0^{(n)} \Omega_0^{(n)} S_0^{(n)}(p^{(n-1)}) \\ &\quad + C_0^{(n)} D_0^{(n)} \tilde{C}_1^{(n)} \tilde{D}_0^{(n)} \Delta_1^{(n)} \Omega_1^{(n)} S_1^{(n)}(q^{(n-1)}) w^{2^{\psi_n}}, \end{aligned} \quad (22)$$

where $p^{(0)} = q^{(0)} = 1$, the operators $C_0^{(n)}(r)$, $D_0^{(n)}(r)$, $\tilde{C}_0^{(n)}(r)$, $\tilde{D}_0^{(n)}(r)$, $\Delta_0^{(n)}(r)$, $S_0^{(n)}(r)$, $\Omega_0^{(n)}(r)$ are equal to r , and the operators $C_1^{(n)}(r)$, $D_1^{(n)}(r)$, $\tilde{C}_1^{(n)}(r)$, $\tilde{D}_1^{(n)}(r)$, $\Delta_1^{(n)}(r)$, $\Omega_1^{(n)}(r)$, $S_1^{(n)}(r)$ are set to $p_{\mathbf{c}_n}(z)r$, $p_{\mathbf{d}_n}(z)r$, $p_{\tilde{\mathbf{c}}_n}(z)r$, $p_{\tilde{\mathbf{d}}_n}(z)r$, and $z^{d_n}r$, $\xi^{\text{j}c_n}r$, and $\xi^{\text{j}\frac{H}{2}}r$, respectively.

By investigating the position of the operators in (22), the configuration vectors, i.e., \mathbf{b}_n^T for $n = 1, 2, \dots, m$, for $C_0^{(n)}(r)$, $D_0^{(n)}(r)$, $\tilde{C}_0^{(n)}(r)$, and $\tilde{D}_0^{(n)}(r)$ are obtained as $[1 \ 0 \ 0 \ 0]$, $[0 \ 1 \ 0 \ 0]$, $[0 \ 0 \ 1 \ 0]$, and $[0 \ 0 \ 1 \ 0]$, respectively. Therefore, by plugging the configuration vectors into (19) and (20), the Boolean functions associated with the construction sequences for $C_0^{(n)}(r)$ are obtained as

$$f_{c,n}(\mathbf{x}) = \begin{cases} (1 - x_{\pi_n}) & n = m \\ (1 - x_{\pi_n})(1 - x_{\pi_{n+1}}) & n < m \end{cases},$$

$$g_{c,n}(\mathbf{x}) = \begin{cases} 0 & n = m \\ (1 - x_{\pi_n})(1 - x_{\pi_{n+1}}) & n < m \end{cases},$$

respectively. Similarly, for $D_0^{(n)}(r)$,

$$f_{d,n}(\mathbf{x}) = \begin{cases} x_{\pi_n} & n = m \\ x_{\pi_n}(1 - x_{\pi_{n+1}}) & n < m \end{cases},$$

$$g_{d,n}(\mathbf{x}) = \begin{cases} 0 & n = m \\ x_{\pi_n}(1 - x_{\pi_{n+1}}) & n < m \end{cases}.$$

For $\tilde{D}_{0,1}^{(n)}(r)$,

$$f_{\tilde{d},n}(\mathbf{x}) = \begin{cases} 0 & n = m \\ (1 - x_{\pi_n})x_{\pi_{n+1}} & n < m \end{cases},$$

$$g_{\tilde{d},n}(\mathbf{x}) = \begin{cases} (1 - x_{\pi_n}) & n = m \\ (1 - x_{\pi_n})x_{\pi_{n+1}} & n < m \end{cases}.$$

For $\tilde{C}_{0,1}^{(n)}(r)$,

$$f_{\tilde{c},n}(\mathbf{x}) = \begin{cases} 0 & n = m \\ x_{\pi_n}x_{\pi_{n+1}} & n < m \end{cases},$$

$$g_{\tilde{c},n}(\mathbf{x}) = \begin{cases} x_{\pi_n} & n = m \\ x_{\pi_n}x_{\pi_{n+1}} & n < m \end{cases}.$$

Therefore, the combined effects of the operators $C_{0,1}^{(n)}(r)$, $D_{0,1}^{(n)}(r)$, $\tilde{C}_{0,1}^{(n)}(r)$, and $\tilde{D}_{0,1}^{(n)}(r)$ on the coefficients of w^x of $p^{(n)}$ and $q^{(n)}$ can be calculated as

$$\begin{aligned} F_{cd\tilde{c}\tilde{d},x}(r) &= r \prod_{n=1}^m p_{c_n}(z)^{f_{c,n}(\mathbf{x})} p_{\tilde{c}_n}(z)^{f_{\tilde{c},n}(\mathbf{x})} \\ &\quad \times p_{d_n}(z)^{f_{d,n}(\mathbf{x})} p_{\tilde{d}_n}(z)^{f_{\tilde{d},n}(\mathbf{x})} \\ &\stackrel{(a)}{=} r \prod_{n=1}^m p_{c_n}(z) f_{c,n}(\mathbf{x}) + p_{\tilde{c}_n}(z) f_{\tilde{c},n}(\mathbf{x}) \\ &\quad \times r p_{d_n}(z) f_{d,n}(\mathbf{x}) + p_{\tilde{d}_n}(z) f_{\tilde{d},n}(\mathbf{x}) \\ &= r \times f_o(\mathbf{x}, z). \end{aligned}$$

and

$$\begin{aligned} G_{cd\tilde{c}\tilde{d},x}(r) &= \prod_{n=1}^m p_{c_n}(z)^{g_{c,n}(\mathbf{x})} p_{\tilde{c}_n}(z)^{g_{\tilde{c},n}(\mathbf{x})} \\ &\quad \times p_{d_n}(z)^{g_{d,n}(\mathbf{x})} p_{\tilde{d}_n}(z)^{g_{\tilde{d},n}(\mathbf{x})} \\ &\stackrel{(b)}{=} \prod_{n=1}^m p_{c_n}(z) g_{c,n}(\mathbf{x}) + p_{\tilde{c}_n}(z) g_{\tilde{c},n}(\mathbf{x}) \\ &\quad \times p_{d_n}(z) g_{d,n}(\mathbf{x}) + p_{\tilde{d}_n}(z) g_{\tilde{d},n}(\mathbf{x}) \\ &= r \times g_o(\mathbf{x}, z), \end{aligned}$$

respectively, where (a) ((b)) is because only one of the functions among $f_{c,n}(\mathbf{x})$, $f_{\tilde{c},n}(\mathbf{x})$, $f_{d,n}(\mathbf{x})$, and $f_{\tilde{d},n}(\mathbf{x})$ ($g_{c,n}(\mathbf{x})$, $g_{\tilde{c},n}(\mathbf{x})$, $g_{d,n}(\mathbf{x})$, and $g_{\tilde{d},n}(\mathbf{x})$) is 1 while the others are equal to 0.

By defining $\omega_n \triangleq \xi^{jc_n}$ and using the identity $\xi^{j\frac{H}{2}} = -1$, the coefficients of w^x of $p^{(n)}$ and $q^{(n)}$ due to the operators $S_{0,1}^{(n)}(r)$, $\Omega_{0,1}^{(n)}(r)$, and $\Delta_{0,1}^{(n)}(r)$ are obtained in [17]. Their compositions can be expressed as

$$F_{comp,x}(r) = G_{comp,x}(r) = r \xi^{jc_i(\mathbf{x})} \times z^{f_s(\mathbf{x})}$$

Finally, by composing $F_{cd\tilde{c}\tilde{d},x}(r)$ and $F_{comp,x}(r)$, and $G_{cd\tilde{c}\tilde{d},x}(r)$ and $G_{comp,x}(r)$, $p_{\mathbf{a}^{(m)}}(z)$ and $p_{\mathbf{b}^{(m)}}(z)$ can be calculated as

$$\begin{aligned} p_{\mathbf{a}^{(m)}}(z) &= p^{(m)} \\ &= \sum_{x=0}^{2^m-1} F_{cd\tilde{c}\tilde{d},x}(F_{comp,x}(r)) w^x \Big|_{r=p^{(0)}=q^{(0)}=1} \\ &= \sum_{x=0}^{2^m-1} f_o(\mathbf{x}, z) \times \xi^{jc_i(\mathbf{x})} \times z^{f_s(\mathbf{x})} \times w^x \end{aligned}$$

and

$$\begin{aligned} p_{\mathbf{b}^{(m)}}(z) &= q^{(m)} \\ &= \sum_{x=0}^{2^m-1} G_{cd\tilde{c}\tilde{d},x}(G_{comp,x}(r)) w^x \Big|_{r=p^{(0)}=q^{(0)}=1} \\ &= \sum_{x=0}^{2^m-1} g_o(\mathbf{x}, z) \times \xi^{jc_i(\mathbf{x})} \times z^{f_s(\mathbf{x})} \times w^x, \end{aligned}$$

respectively, where w can be chosen arbitrarily as $w = z^U$.

The sequences $\mathbf{a}^{(m)}$ and $\mathbf{b}^{(m)}$ construct a GCP based on (21). Since the phase rotation does not change the APAC of

a sequence, the sequences $\mathbf{a}^{(m)} \times \xi^{jc'}$ and $\mathbf{b}^{(m)} \times \xi^{jc''}$ also construct a GCP. \square

REFERENCES

- [1] A. Ajiaz, H. Aghvami, and M. Amani, "A survey on mobile data offloading: technical and business perspectives," *IEEE Wireless Commun.*, vol. 20, no. 2, pp. 104–112, Apr. 2013.
- [2] ETSI, "5 GHz RLAN; harmonized EN covering the essential requirements of article 3.2 of the directive 2014/53/eu," EN 301 893, May 2017.
- [3] Ericsson, "UL signals and channels for NR-U," R1-1900997, Jan. 2019.
- [4] S. Gokceli, T. Levanen, T. Riihonen, M. Renfors, and M. Valkama, "Frequency-selective PAPR reduction for OFDM," *CoRR*, vol. abs/1902.07466, Apr. 2019.
- [5] Y. Rahmatallah and S. Mohan, "Peak-to-average power ratio reduction in OFDM systems: A survey and taxonomy," *IEEE Commun. Surveys Tut.*, vol. 15, no. 4, pp. 1567–1592, Fourth 2013.
- [6] S. H. Muller and J. B. Huber, "OFDM with reduced peak-to-average power ratio by optimum combination of partial transmit sequences," *Electronics Letters*, vol. 33, no. 5, pp. 368–369, Feb. 1997.
- [7] X. Huang, J. Lu, J. Zheng, K. B. Letaief, and J. Gu, "Companding transform for reduction in peak-to-average power ratio of OFDM signals," *IEEE Trans. Wireless Commun.*, vol. 3, no. 6, pp. 2030–2039, Nov. 2004.
- [8] H. Sari, G. Karam, and I. Jeanclaude, "Transmission techniques for digital terrestrial TV broadcasting," *IEEE Commun. Mag.*, vol. 33, no. 2, pp. 100–109, Feb. 1995.
- [9] A. Sahin, R. Yang, F. LaSita, and R. L. Olesen, "A comparison of SC-FDE and UW DFT-s-OFDM for millimeter wave communications," in *Proc. IEEE International Communications Conference*, May 2018.
- [10] A. Sahin, R. Yang, E. Bala, M. C. Beluri, and R. L. Olesen, "Flexible DFT-S-OFDM: Solutions and challenges," *IEEE Commun. Mag.*, vol. 54, no. 11, pp. 106–112, Nov. 2016.
- [11] A. E. Jones, T. A. Wilkinson, and S. K. Barton, "Block coding scheme for reduction of peak to mean envelope power ratio of multicarrier transmission schemes," *Electronics Letters*, vol. 30, no. 25, pp. 2098–2099, Dec. 1994.
- [12] A. E. Jones and T. A. Wilkinson, "Combined coding for error control and increased robustness to system nonlinearities in OFDM," in *IEEE Vehicular Technology Conference*, vol. 2, Apr. 1996, pp. 904–908.
- [13] O. Daoud and O. Alani, "Reducing the PAPR by utilisation of the LDPC code," *IET Communications*, vol. 3, no. 4, pp. 520–529, Apr. 2009.
- [14] Y. Tsai, S. Deng, K. Chen, and M. Lin, "Turbo coded OFDM for reducing PAPR and error rates," *IEEE Trans. Wireless Commun.*, vol. 7, no. 1, pp. 84–89, Jan. 2008.
- [15] M. Golay, "Complementary series," *IRE Trans. Inf. Theory*, vol. 7, no. 2, pp. 82–87, Apr. 1961.
- [16] J. A. Davis and J. Jedwab, "Peak-to-mean power control in OFDM, Golay complementary sequences, and Reed-Muller codes," *IEEE Trans. Inf. Theory*, vol. 45, no. 7, pp. 2397–2417, Nov. 1999.
- [17] A. Sahin and R. Yang, "A generic complementary sequence encoder," *CoRR*, vol. abs/1810.02383v2, Aug. 2019.
- [18] 3GPP, "Physical channels and modulation (Release 15)," TS 38.211 V15.5.0, Mar. 2019.
- [19] A. Sahin and R. Yang, "A reliable uplink control channel design with complementary sequences," in *Proc. IEEE International Communications Conference*, May 2019.
- [20] S. Boyd, "Multitone signals with low crest factor," *IEEE Trans. Circuits Syst.*, vol. 33, no. 10, pp. 1018–1022, Oct. 1986.
- [21] M. G. Parker, K. G. Paterson, and C. Tellambura, "Golay complementary sequences," in *Wiley Encyclopedia of Telecommunications*, 2003.
- [22] J. J. Benedetto, I. Konstantinidis, and M. Rangaswamy, "Phase-coded waveforms and their design," *IEEE Signal Processing Magazine*, vol. 26, no. 1, pp. 22–31, Jan. 2009.
- [23] S. Sesia, I. Toufik, and M. Baker, *LTE, The UMTS Long Term Evolution: From Theory to Practice*. Wiley Publishing, 2009.
- [24] R. Turyn, "Hadamard matrices, Baumert-Hall units, four-symbol sequences, pulse compression, and surface wave encodings," *Journal of Combinatorial Theory, Series A*, vol. 16, no. 3, pp. 313–333, 1974.
- [25] E. Garcia, J. J. Garcia, J. U. A. M. C. Perez, and A. Hernandez, "Generation algorithm for multilevel LS codes," *Electronics Letters*, vol. 46, no. 21, pp. 1465–1467, Oct. 2010.

- [26] K. G. Paterson, "Generalized Reed-Muller codes and power control in OFDM modulation," *IEEE Trans. Inf. Theory*, vol. 46, no. 1, pp. 104–120, Jan. 2000.
- [27] W. H. Holzmann and H. Kharaghani, "A computer search for complex Golay sequences," *Aust. Journ. Comb.*, vol. 10, pp. 251–258, Apr. 1994.
- [28] K. . Schmidt and A. Finger, "Simple maximum-likelihood decoding of generalized first-order Reed-Muller codes," *IEEE Communications Letters*, vol. 9, no. 10, pp. 912–914, Oct. 2005.
- [29] Ericsson, "UL signals and channels for NR-U," R1-1907453, May 2019.
- [30] Ericsson, Nokia, Lenovo, LG, and ZTE, "WF on DMRS multi-tone evaluation methods," R1-163437, Apr. 2016.